Influence of Terminal Hydrophobe Branching on the Aqueous Solution Behavior of Model Hydrophobically Modified Ethoxylated Urethane Associative Thickeners†

Peter T. Elliott, Lin-lin Xing, Wylie H. Wetzel, and J. Edward Glass*

Polymer and Coatings Department, North Dakota State University, Fargo, North Dakota 58103

Received February 1, 2002; Revised Manuscript Received March 21, 2003

ABSTRACT: The influence of terminal hydrophobe branching on the micellar properties of *H*ydrophobically modified *E*thoxylated *UR*ethanes (HEURs) is addressed through fluorescence, dynamic light scattering (DLS), solution rheology, and Raman spectroscopy. Model HEURs used in this study are monodisperse and fully substituted with hydrophobic groups of different structures. Two linear hydrophobes (*l*-$C_{12}H_{25}$ and *l*-$C_{16}H_{33}$) and three branched hydrophobes [*b*-($C_{12}H_{26}$), *b*-($C_{16}H_{34}$), and *b*-($C_{20}H_{42}$)] are coupled to the hydroxyls of POE_{670} and POE_{195} through 4,4-methylene bis(dicyclohexyl)diisocyanate (H_{12}MDI) units. Prior low molecular weight surfactant studies observed that a CH_2 group, introduced as a branch from a linear hydrophobe, contributes approximately half to the surfactant's hydrophobicity that the same CH_2 unit would add to the linear chain. Within hydrophobe equivalent comparisons, greater hydrophobic domains are indicated in pyrene's I_1/I_3 emission ratio for the linear hydrophobe HEURs, denoting a more hydrophilic core in branched HEURs. An increase in the number of $-CH_2-$ groups notably influences aqueous solution viscosities, as expected, but among equivalent hydrocarbon comparisons, the moderate-size linear hydrophobe is more viscosifying than the branched hydrophobe at high concentrations. Viscosity increases correlate with the aggregation sizes estimated from DLS studies as aggregate sizes approach 500 nm, covering small to large hydrophobes and different oxyethylene spacer lengths. Conformational differences (Raman spectroscopy) of poly(oxyethylenes) and HEURs under stagnant and flow conditions are also examined. The presence of byproduct impurities can markedly influence these results.

Introduction

Surfactant-modified, water-soluble polymers (W-SPs) offer several advantages over nonmodified W-SPs in a number of applications. The advantages include changes in rheological profiles (e.g., controlled viscosities at low shear rates without large elastic responses at high deformation rates) and the ability to stabilize disperse phases through competitive adsorption in an environment containing surfactant. Much of the history and progress in this area have been described in the introduction of a previous article,[1] in the last of several *Advances in Chemistry* books,[2] and in a recent review article.[3] Of the compositional possibilities available in surfactant-modified W-SPs, only the *H*ydrophobically modified, *E*thoxylated *UR*ethanes (HEURs), if prepared by a non-step-growth synthesis, offer the clarity of composition needed in model studies.

Our prior HEUR studies have included examination of different geometries with short oxyethylene spacings,[4,5] linear polymers with variable terminal hydrophobe sizes separated by larger ethoxylate spacings,[6] and the influence of broad molecular weight distributions with different terminal hydrophobe sizes. The latter mixtures also contain underivatized oxyethylene components.[1,7,8] The current contribution examines the influence of branching of the terminal hydrophobes on micellar behavior and solution rheology. To place these studies in perspective, the prior observations in low molecular weight branched surfactants are reviewed below.

* To whom correspondence should be addressed. E-mail: eglass@fargocity.com.

† Originally presented at the National Meeting of the American Chemical Society, Boston, MA, 1998, Colloid Division.

Prior Conventional Surfactant Studies. In one of the first branched surfactant studies,[9] Wade's group observed that surfactant structure among ethoxylated alkyl phenols had a significant effect on the solubility and on the interfacial tension of microemulsions. If the hydrophilic and lipophilic moieties of the surfactant were increased simultaneously via hydrophobe branching in concert with the correct ethoxylation level,[10,11] surfactant groupings were obtained that exhibited optimum behavior in microemulsions.

In studies reported[12,13] from Exxon's laboratories, hydrocarbon chain branching resulted in a higher critical micelle concentration (cmc), and was attributed to steric hindrance to aggregation. For example, the cmc of branched sodium dodecyl sulfate (*b*-SDS) was observed to be ∼2 times higher than the linear analogue (SDS), but was 1 order of magnitude lower than that of sodium octyl sulfate. The introduction of chain branching also influenced the equilibrium surface tension and effectiveness in reducing the dynamic surface tension at the air−water interface. Branched surfactants should therefore offer an advantage in reduced foaming in surfactant applications.

In branched sulfate and ethoxy sulfate surfactants, hydrocarbon chain packing, probed in water and 0.1 N NaCl solutions, revealed differences[14] in the microstructures of micellar aggregates (FTIR and fluorescence, 15−50 °C). The micellar microstructure of the beta-branched hydrophobes is sensitive to electrolyte addition but insensitive to temperature, while that of the linear hydrophobe is insensitive to electrolyte addition but sensitive to temperature. The micropolarity of aqueous micellar solutions of ethoxylates, sodium ethoxy sulfates, and sulfates derived from linear and branched

10.1021/ma020166f CCC: $25.00
Published on Web 10/09/2003

hydrocarbon alcohols also were investigated,[15] using a solvatochromic pyridinio-*N*-phenoxide betaine, ET-30, polarity probe. Branching of the hydrophobe resulted in a more porous micellar aggregate. Increasing the temperature was observed to expel water from the hydrophobic regions of the aggregates and decrease the effective micropolarity in linear and branched surfactants.

In the discussions to follow the influence of terminal hydrophobe branching on the micellar properties of *H*ydrophically modified *E*thoxylated *UR*ethanes (HEURs) are addressed through fluorescence, dynamic light scattering, and solution rheology. The model HEUR thickeners used in this study are monodisperse and fully substituted with hydrophobic groups of different structures. Two linear hydrophobes (*l*-$C_{12}H_{25}$ and *l*-$C_{16}H_{33}$) and three branched hydrophobes (*b*-($C_{12}H_{26}$), *b*-($C_{16}H_{34}$), and *b*-($C_{20}H_{42}$)) are coupled to the hydroxyls of POE_{670} and POE_{195} through 4,4-methylene bis(dicyclohexyl)-isocyanate ($H_{12}MDI$) units. It has been delineated in conventional surfactant studies that a CH_2 group, introduced as a branch from a linear hydrophobe, contributes to the surfactant's hydrophobicity approximately half that of the same CH_2 unit added to the linear chain.[13−16] An ideal comparison, therefore, would be between a linear-$C_{12}H_{25}$ and a di-C_8H_{17} (i.e., branched-$C_{16}H_{34}$), or between a linear-$C_{15}H_{31}$ and a di-$C_{10}H_{21}$ (i.e., branched-$C_{20}H_{42}$). The linear $C_{15}H_{31}OH$ precursor was not readily available, so the later comparison is made with a linear-$C_{16}H_{33}OH$ adduct to the HEUR chain.

Experimental Section

Materials. The molecular weights of the poly(oxyethylenes) (POEs) obtained from Union Carbide and Fluka were reported to be 35 000 and 8000, respectively. Hydroxyl number titrations were performed according to the pyromellitic dianhydride/imidazole method[17] to accurately determine the molecular weights. $H_{12}MDI$, supplied by Miles, was gravity filtered before use. Isocyanate numbers were determined using dibutylamine and back-titrating to obtain the concentration of isocyanate. Toluene and tetrahydrofuran (THF) were distilled and kept dry over molecular sieves before use. Water used for viscosity measurements was passed through a Milli-Q (Millipore) ion exchange column and distilled from $KMnO_4$ solutions. Dibutyltin dilaurate (95%) was obtained from Aldrich and used as received. The hydrophobes (1-dodecanol, 1-hexadecanol, dihexylamine, dioctylamine, and didecylamine) obtained from Aldrich were used as received.

Synthesis of Hydrophobe Modified Poly(oxyethylene). The following thickeners are described as uni-HEURs to signify that they are not made by a classic step-growth reaction that produces broad molecular weight distributions. The synthesis procedure follows those previously described[1,4,5] (excluding the step-growth synthesis also used in ref 1). The reaction sequence uses an excess of diisocyanate to avoid chain extension (Scheme 1; stirred for 4 h at 45−50 °C). Their molecular weights are given in Table 1. The thickeners were purified by dissolution in hot acetone, gravity filtration, and precipitation in petroleum ether. This procedure was typically done three times to remove excess diurea and diurethane products due to the excess of diisocyanate. In these syntheses there is an excess of the diisocyanate that will react with the excess of hydrophobe added to produce byproducts (e.g., a diurea if the second adduct is the branched hydrophobic amine or a diurethane if the second adduct is a hydrophobic alcohol). The diurethane byproduct is not removed without the final methanol extraction and reprecipitation in petroleum ether. This difference is important in obtaining clear aqueous solutions.

Fluorescence. The quencher, benzophenone (+99%), was used as received from Aldrich. The probe, pyrene (+98%, Aldrich), was purified by recrystallization (two times) from absolute ethanol. Solutions for critical aggregate concentration (cac) measurements were prepared according to the following procedure. The surfactant or thickener solution was weighed into a 20-mL vial and diluted to a 1 g total weight with distilled water. This solution was diluted to 10 g with the filtered pyrene-saturated solution, so that the concentration of pyrene was kept constant and less than 10^{-6} M. Solutions for quenching experiments were prepared as follows. A thickener stock solution was prepared by dissolving the powder in pyrene-saturated water and rolled in the dark for 24 h. A portion of these solutions was saturated with benzophenone, and the mixtures were put on the roller in the dark for 24 h. After centrifugation or filtration, aliquots of the benzophenone-saturated solutions were prepared in the concentration range of 0 to 2×10^{-4} M, and then added to the thickener/pyrene solutions. The UV absorption spectra were recorded with a Hewlett-Packard 8450A diode array spectrometer. Steady-state fluorescence spectra were recorded on a SPEX 2T2

Scheme 1. Synthesis of Narrow Molecular Weight Hydrophobically Modified, Ethoxylated Urethane (HEUR) Associative Thickeners

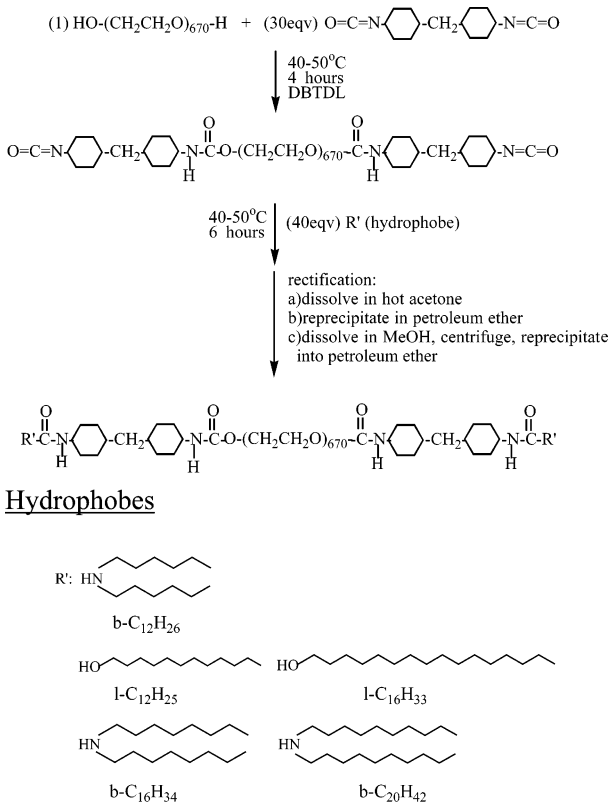

Table 1. Characterization of Model HEURs

thickener	M_w	M_n	M_w/M_n[a]	% hydrophobe substn (±4.0%)[b]
(*b*-($C_{12}H_{26}$)/$H_{12}MDI$)$_2EO_{670}$	29 300	25 600	1.1	100
(*b*-($C_{12}H_{26}$)/$H_{12}MDI$)$_2EO_{195}$	8 200	6 600	1.2	95
(*l*-($C_{12}H_{25}$)/$H_{12}MDI$)$_2EO_{670}$	28 300	25 000	1.1	96
(*l*-($C_{12}H_{25}$)/$H_{12}MDI$)$_2EO_{195}$	6 700	5 800	1.1	96
(*b*-($C_{16}H_{34}$)/$H_{12}MDI$)$_2EO_{670}$	28 700	24 300	1.2	96
(*b*-($C_{16}H_{34}$)/$H_{12}MDI$)$_2EO_{195}$	8 000	7 000	1.1	95
(*b*-($C_{20}H_{42}$)/$H_{12}MDI$)$_2EO_{670}$	28 800	24 700	1.2	98
(*b*-($C_{20}H_{42}$)/$H_{12}MDI$)$_2EO_{195}$	7 100	6 100	1.2	94
(*l*-($C_{16}H_{33}$)/$H_{12}MDI$)$_2EO_{670}$	29 300	25 400	1.2	95
(*l*-($C_{16}H_{33}$)/$H_{12}MDI$)$_2EO_{195}$	7 000	5 900	1.2	94

[a] The molecular weight distribution data were determined from GPC measurements.[1,5,7] [b] ^1H NMR of the modified POEs were recorded using a JEOL GSX-270 MHz Fourier transform NMR spectrometer with deuterated chloroform as the solvent and 1,4-diflorobenzene as the standard for quantitative measurements.

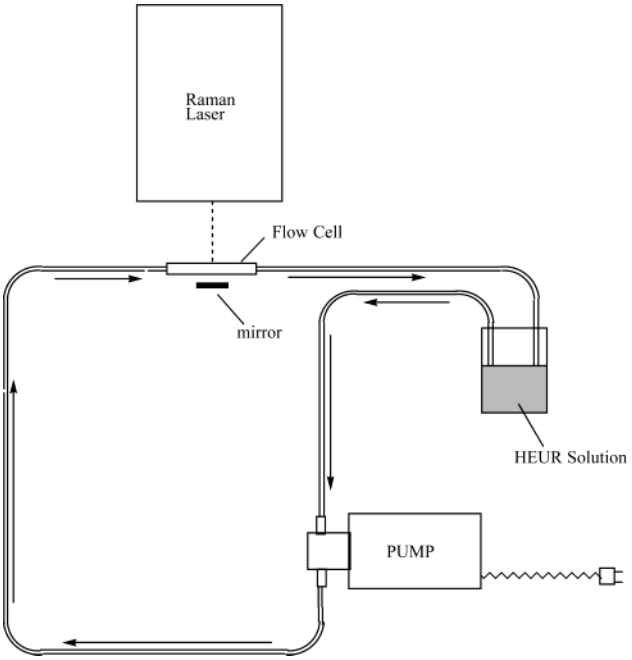

Figure 1. Raman flow cell.

Fluorolog fluorometer using a xenon lamp as the light source and equipped with a DM3000F data system.

Fluorescence emission spectra (λ = 350−450 nm) were recorded at room temperature for the probe (pyrene). The excitation wavelength was set at 334, nm and the bandwidths were set to 3 nm for excitation and 1.5 nm for emission. The intensity ratios at the first vibronic peak (λ = 372 nm) and at the third vibronic peak (λ = 383 nm) in the pyrene emission spectra, I_1/I_3, were used to determine the cac of the thickeners. In the determination of a mean aggregation number, N, the ratios of fluorescence intensities in the absence and presence of quencher (benzophenone) were calculated as the ratios of the integrated spectral areas (in wavelength units, from 350 to 450 nm).

Dynamic Light Scattering and Rheology. Particle size measurements were performed on a NICOMP 370 dynamic light scattering instrument from Particle Sizing Systems. Diffusion coefficients (D) were extracted from the fluctuating light scattering signal through an autocorrelation function, and then used to determine particle size (R) through the Stokes−Einstein equation ($D = kT/6\pi\eta R$). Either a Gaussian or NICOMP (inverse LaPlace transform) distribution analysis was used depending on if the particle size distribution was unimodal or bimodal, respectively. All solutions were filtered (1000 nm) prior to examination and run at 25 °C. To all HEUR solutions 2 mM SDS was added to obtain solubility.

Steady state, low shear rate viscosities were measured using a Brookfield cone and plate viscometer. Ramped viscosity profiles (6 min) and oscillatory measurements were recorded using a Carri-Med controlled stress rheometer (4 cm with a 2 °C cone angle and a double concentric cylinder geometry (R_1 = 20.00 mm, R_2 = 20.38 mm, R_3 = 21.96 mm, cylinder height = 20.50 mm, for low viscosity solutions).

In both the DLS and fluorescence studies there are many assumptions in interpreting the results with HEUR solutions, which are questionable as the viscosity is increased with increasing hydrophobe size.

Raman Spectroscopy. Raman Spectra were run on a Bruker Equinox 55 FRA106 Raman module system equipped with a Nd:YAG laser, CaF_2 beam splitter, and a Ge detector. The spectral resolution was set to 4. The laser was operated at 560 mW power for 2000 scans at 4 kHz scan velocity. Samples were passed through a homemade flow cell (Figure 1) with a mirror backing for increased signal-to-noise ratio. All samples were run at room temperature (25 °C).

Results and Discussion

Fluorescence. A. Examination of Hydrophobe Structure on Critical Aggregation Concentrations (cac's). The I_1/I_3 intensity ratios for pyrene fluorescence as a function of model HEUR concentrations are illustrated in Figure 2. In contrast to the sharp decrease in the pyrene emission ratio, I_1/I_3, in normal aqueous surfactant (i.e., SDS or Triton X-100) solutions, the I_1/I_3 transition for the HEUR solutions (using the low EO spacer length to minimize solution viscosities) occurs over a broad concentration range (10^{-7} to 2×10^{-5} M). A gradual formation of hydrophobic domains, beginning with dimers, trimers, etc., is responsible for the gradual association. The critical aggregation concentration (cac) of model HEURs is taken in this study as the inflection point in the I_1/I_3 ratio as it enters the plateau at higher concentrations, 2 ($\pm$1) $\times$ 10^{-5} M. Short EO spacing, $HEUR_{195}$, derivatives are emphasized in most of our fluorescence studies to avoid viscosity distortion of the fluorescence responses at the higher HEUR concentrations. Among the linear HEURs, the l-$C_{16}H_{33}$ has a

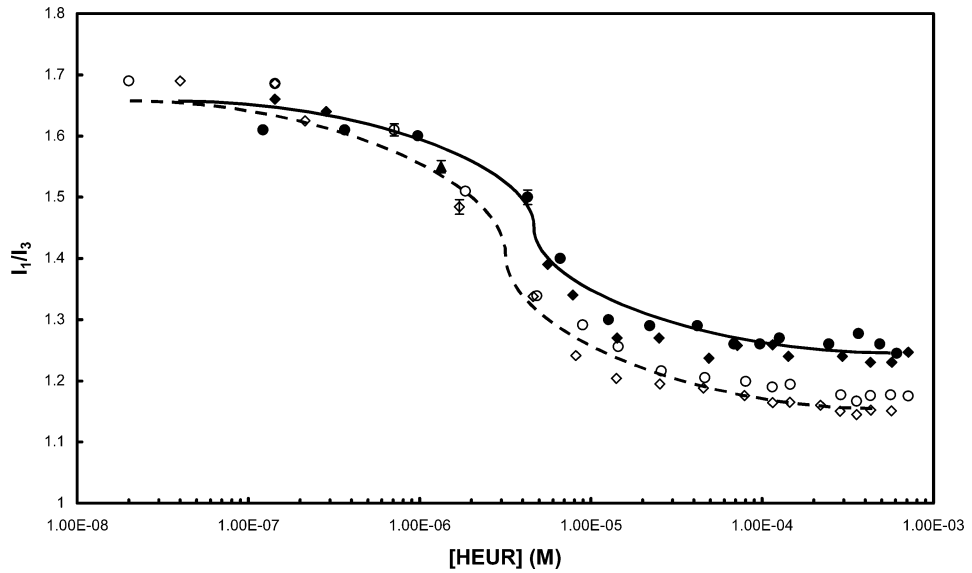

Figure 2. Dependence of I_1/I_3 pyrene ratio on $H_{12}MDI-HEUR_{195}$, with structurally different hydrophobes, aqueous solution concentration. Hydrophobe symbols: (●) b-$C_{12}H_{26}$; (◆) b-$C_{16}H_{34}$; (○) l-$C_{12}H_{25}$; (◇) l-$C_{16}H_{33}$. The b-$C_{20}H_{42}$ data are omitted for clarity.

lower cac than the *l*-$C_{12}H_{25}$ HEUR, and the same can be said for the branched hydrophobe HEURs with increasing carbon content (Figure 2). With a change in the number of CH_2 groups the changes in the fluorescence spectra could be related to the viscosity behavior of the materials within each series. The *b*-$C_{20}H_{42}$−HEUR data are approximate with the *l*-$C_{12}H_{25}$ data and are omitted for clarity, but this pair emphasizes a lack of comparative difference detracting from the fluorescence cac−viscosity relationship: the former is far more viscosifying than the latter, and this is not reflected in the fluorescence data. The differences in the fluorescence data may in part reflect the relative solubility of pyrene in the different hydrophobic domains,[18] indicating that the branched hydrophobes provide a more hydrophilic environment. Corresponding data with larger EO spacings also were run, with general agreement but with wider variations.

B. Mean Aggregation Number, *N*, in Model HEUR Aqueous Solutions at 1.77 × 10^{-4} M. The mean aggregation number, *N*, represents the mean number of surfactant monomers in a micelle or of chain ends in an HEUR aggregate. Since fluorescent probe techniques are more reliable for the determination of *N* due to their insensitivity to intermicellar interactions and straightforward data processing,[19,20] these methods have been employed, in many studies, in preference to a number of classical colloidal measurements, such as light scattering, X-ray scattering, and gel filtration. In this study, the steady-state fluorescence method with pyrene as the luminescent probe and benzophenone as the quencher has been used. This method proposed by Turro and Yekta for anionic micelles[21] has been extended to cationic and nonionic micelles[22] and to polymer−surfactant[23−28] systems.

The relative fluorescence intensity of a probe is related to the quencher concentration [Q] and the micelle concentration [M] by the expression

$$\ln(I_0/I_q) = [Q]/[M] \quad (1)$$

where I_0 is the emission intensity in the absence of quencher and I_q is the emission intensity in the presence of quencher. The slope of $\ln(I_0/I_q)$ vs [Q] yields the micelle concentration [M]. The micelle aggregation number N_s is determined from

$$N_s = (S - \text{cmc})/[M] \quad (2)$$

where *S* is the total surfactant concentration in the solution and cmc is the critical micelle concentration.

For HEUR solutions, the aggregation number *N* can be determined from

$$N = (C_p - \text{cac})/[M] \quad (3)$$

where C_p is the hydrophobe group molar concentration and cac is the critical aggregation concentration of model HEUR aqueous solutions.

Although the steady-state fluorescence quenching method has been criticized for underestimating aggregation numbers when materials such as salts are added to the systems,[19,29,30] this method is used to determine *N* when the experimental conditions are chosen with care.[24,31,32] The pair, pyrene/benzophenone, used in this study nearly satisfies the conditions.[25,32,33] The steady-state fluorescence quenching method yields consistent *N* values for surfactant−polymer solutions with those obtained using time-resolved fluorescence or other techniques.[34−36]

Table 2. Aggregation Numbers of Model HEUR Aqueous Solutions at 1.77 × 10^{-4} M

thickener[a]	[M] × 10^5 (M)	*N* (±1)
(*b*-($C_{12}H_{26}$)/H_{12}MDI)$_2$EO_{670}	7.0	5
(*b*-($C_{12}H_{26}$)/H_{12}MDI)$_2$EO_{195}	6.1	6
(*l*-($C_{12}H_{25}$)/H_{12}MDI)$_2$EO_{670}	6.0	6
(*l*-($C_{12}H_{25}$)/H_{12}MDI)$_2$EO_{195}	5.3	7
(*b*-($C_{16}H_{34}$)/H_{12}MDI)$_2$EO_{670}	7.3	5
(*b*-($C_{16}H_{34}$)/H_{12}MDI)$_2$EO_{195}	6.2	6
(*b*-($C_{20}H_{42}$)/H_{12}MDI)$_2$EO_{670}	5.9	6
(*b*-($C_{20}H_{42}$)/H_{12}MDI)$_2$EO_{195}	5.3	7
(*l*-($C_{16}H_{33}$)/H_{12}MDI)$_2$EO_{670}	6.6	5
(*l*-($C_{16}H_{33}$)/H_{12}MDI)$_2$EO_{195}	4.8	7

[a] For dissolution in water, all aqueous solutions of fully modified model HEURs were prepared with the addition of 0.1 mM SDS. The cmc of SDS is 8.2 mM.

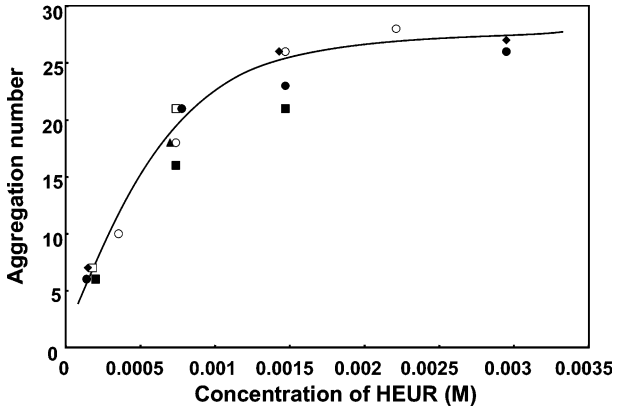

Figure 3. Aggregation number dependence on concentration of HEURs with POE_{195} spacings. Hydrophobe symbols: (○) *l*-$C_{12}H_{25}$; (□) *l*-$C_{16}H_{33}$; (●) *b*-$C_{12}H_{26}$; (◆) *b*-$C_{16}H_{34}$; (■) *b*-$C_{20}H_{42}$.

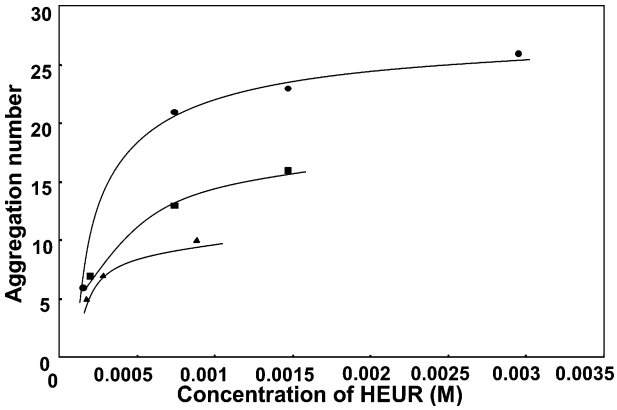

Figure 4. Aggregation number dependence on concentration of *b*-$C_{12}H_{26}$ H_{12}MDI−HEURs with different EO lengths. Symbols: (●) POE_{195} spacer; (■) POE_{270}; (▲) POE_{670} spacer.

A linear dependence of $\ln(I_0/I_q)$ on quencher concentration is observed for [Q]/[M] ≤ 2. Since the data points correspond to a best-fit linear curve, the Poisson statistics assumed in the derivation of eqs 2 and 3 are assumed valid.[21] To compare the aggregation numbers among the model HEURs with different oxyethylene (EO) spacer lengths and different terminal hydrophobe groups, the concentration for all model HEUR solutions is kept at 1.77 × 10^{-4} M, approximately 10 times their cac, but at a concentration where solution viscosities are low. The aggregation numbers of all model HEUR aqueous solutions at 1.77 × 10^{-4} M are summarized in Table 2. Within experimental error there is no differ-

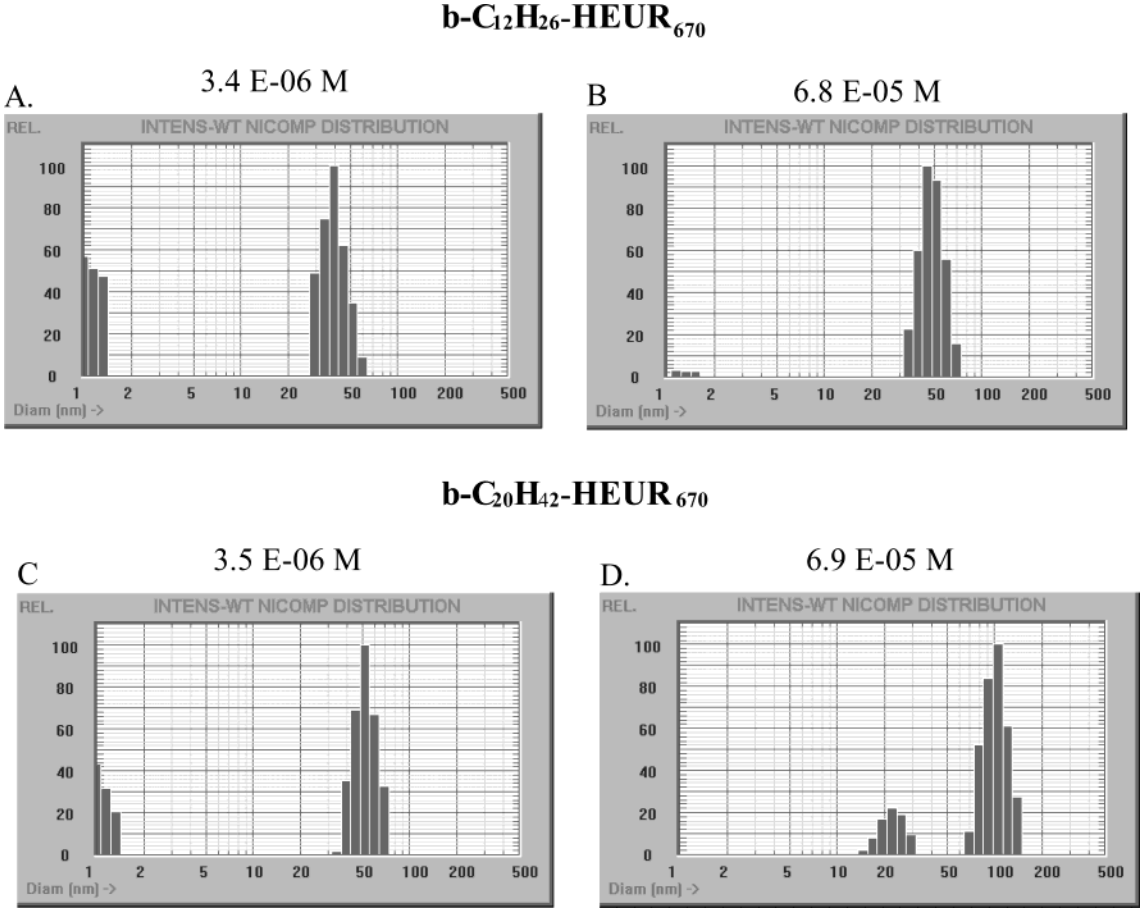

Figure 5. Median aggregate sizes for aqueous R−H_{12}MDI−$HEUR_{670}$ solutions at low concentrations.

ence. Until recently essentially all of the aggregation numbers, determined on well-defined materials, were on one type of thickener: the *l*-$C_{12}H_{25}$ hydrophobe linked to a POE by only an ether linkage. Although all of the hydrophobes in the current study are significantly more hydrophobic than the ether linked $C_{12}H_{25}$ material, because of the H_{12}MDI linkage, the aggregation numbers listed above are in general agreement with the previously values of J. Francois and co-workers.[37]

Although the differences are small (Table 2), there appear on average to be a higher aggregation number with the smaller EO spacing in this study. This would be consistent with the prior studies for the intrahydrophobe associations of POE_{100} and POE_{200} with terminal pyrene groups.[38] In the POE_{670} molecular weight range coupled with octadecyl and hexadecyl monoisocyanate, Russel and co-workers,[39] using dynamic light scattering (DLS) and intrinsic viscosities, have reported aggregation numbers (N) of 33 and 20. Using fluorescence studies Winnik's group observed the N values of these compounds, at concentrations significantly higher than those in Table 2, to be half the values determined by the DLS/intrinsic viscosity approach. Considering the differences in viscosity efficiencies and aggregate size variations with increasing hydrophobe size (DLS discussed below), the lack of variation in N values in Table 2 is surprising, but the extent of association is dependent on concentration and, in this study, on the concentration selected as the cac.

The mean aggregation numbers as a function of HEUR concentration for different hydrophobe sizes in the R−$HEUR_{195}$ family are illustrated in Figure 3. The data in Figure 2 provide a more meaningful projection that a difference in viscosity will occur with increasing hydrophobe size; this is related to our selection of the upper inflection point in Figure 2. The simple analysis reflected in the magnitude of the I_1/I_3 ratio, given a variation related to the hydrophobicity of the core (linear vs branched), is more reflective of the data in the following sections.

Finally, in the earlier fluorescence study, the aggregation behavior of the *l*-$C_{12}H_{25}$ connected to POE by an ether unit (Williamson synthesis) was dependent on the POE spacer length up to 450 EO units.[37] The data in Figure 4 for the least hydrophobic terminal group in this study, *b*-$C_{12}H_{26}$, observed that the aggregation numbers increase with decreasing EO lengths, in agreement with the prior study. There are viscosity limitations with the larger hydrophobes that are connected to POE by a hydrophobic diisocyanate in this study that limit the upper concentrations that can be used. Even at lower concentrations, smaller viscosity differences may be restrictive in data interpretations because of the assumptions needed in data interpretation.

C. Dynamic Light Scattering (DLS). Calculations of the size of POE_{670} and POE_{195} from an equation using weight-average molecular weights[40] provide a diameter size of 5.1 and 2.6 nm, respectively. In this study the number-average molecular weight would be more appropriate. The experimental values determined with a Nicomp 370 dynamic light scattering device provide a median value of 1.4 nm. Many assumptions in this and in the fluorescence technique are required to compare the results with the rheology data in the next section.

The emphasis in this phase of our study is on two branched hydrophobes at the viscosify extremes:

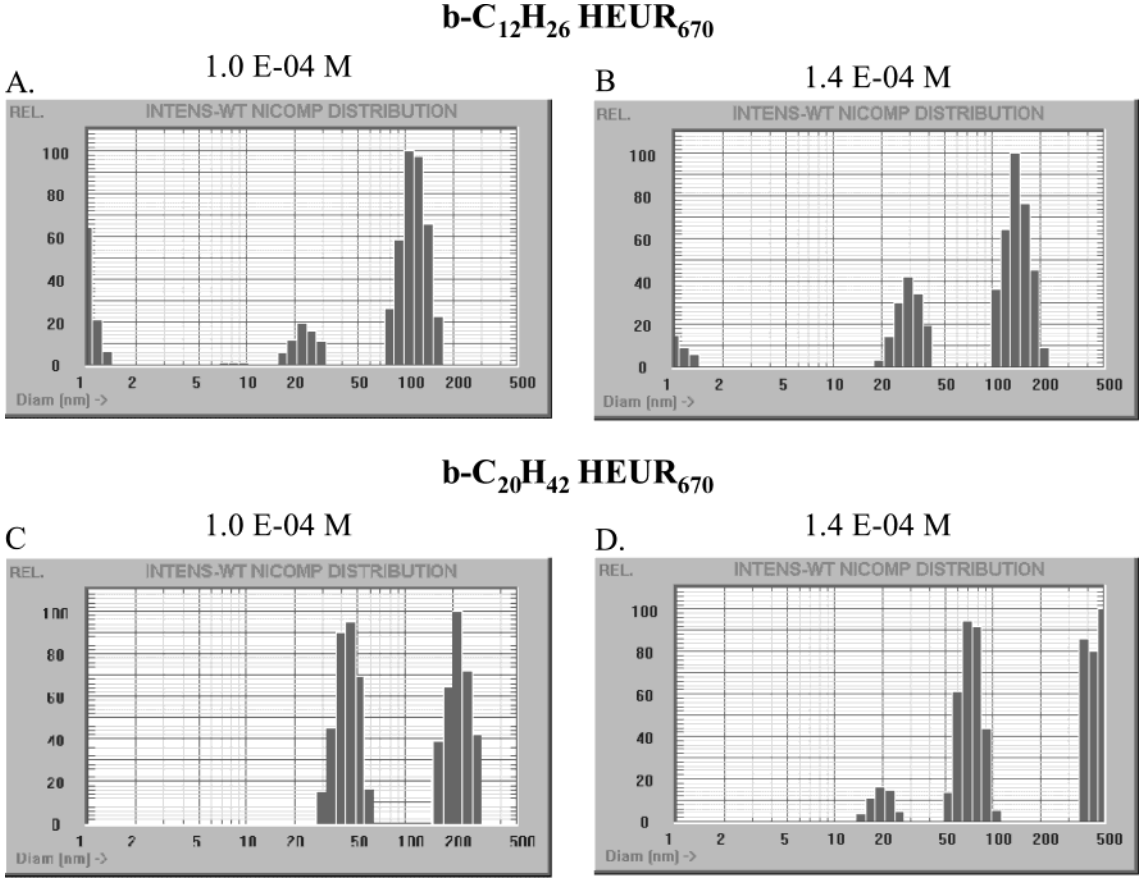

Figure 6. Median aggregate sizes for aqueous R−H_{12}MDI−$HEUR_{670}$ solutions at higher concentrations.

b-$C_{12}H_{26}$−H_{12}MDI and *b*-$C_{20}H_{42}$−H_{12}MDI. The pyrene emission ratio, I_1/I_3, begins to fall for both HEURs around 10^{-7} M. Slightly above this concentration (3.4 $\times$ 10^{-6} M), the smaller hydrophobe with the largest EO spacer, (*b*-$C_{12}H_{26}$−H_{12}MDI)$_2$−$HEUR_{670}$, solutions exhibit two median sizes (Figure 5A). The larger median size of 40 nm is a grouping of hydrophobe associations that represent an aggregation size in excess of a flowered micelle. In the most recent publication on HDU and ODU[39] HEURs, the authors conclude that the micelle radii are 17 and 20 nm, respectively. The H_{12}-MDI coupler used in this study accounts for our values being double the HDU and ODU values. In the past decade there has been no examination of H_{12}MDI in HEUR thickeners, but it is the commercial diisocyanate of choice because of its hydrophobicity. Another possibility for the difference is the addition of small amounts of sodium dodecyl sulfate to all narrow molecular weight model HEURs. We have taken this approach since 1989[4] to avoid phase separation in all of our model HEUR studies. With increasing concentration (up to 6.8 $\times$ 10^{-5} M, 0.2 wt %, Figure 5B) a modest increase in size to 50 nm is observed with concentration increases. When the considerably more hydrophobic thickener, *b*-$C_{20}H_{42}$−H_{12}MDI−$HEUR_{670}$, is examined in this concentration range, the median size of the associative aggregate is larger (Figure 5C,D) at the higher concentration. As the number of aggregates grow, the possibility of interbridging increases, complemented by a greater residence time of the associations of the larger hydrophobe. At 0.2 wt %, the larger hydrophobe aggregate size is observed as a bimodal distribution at 6.9 $\times$ 10^{-5} M (Figure 5D), with median sizes of 20 and 100 nm.

This bimodal distribution of aggregates is observed with the smaller hydrophobe at a higher concentration, 1.02 $\times$ 10^{-4} M (0.3 wt %, Figure 6A). Both median sizes in this distribution increase in size as the concentration is increased to 1.37 $\times$ 10^{-4} M (0.4 wt %, Figure 6B). With the larger more hydrophobic species, *b*-$C_{20}H_{42}$−$HEUR_{670}$, at the higher concentrations (Figure 6C and D), the median aggregate sizes are larger than observed with the smaller hydrophobe *b*-$C_{12}H_{26}$−$HEUR_{670}$. At 1.39 $\times$ 10^{-4} M (0.4 wt %), *b*-$C_{20}H_{42}$−$HEUR_{670}$ exhibits a trimodal distribution (Figure 6D) with the largest median aggregate size of 500 nm. No sizes larger than this median were observed, so the ordinate was held at 500 nm to conform with the other DLS data. It is at this concentration that the viscosity begins to dramatically increase (discussed in the next section) in *b*-$C_{20}H_{42}$−$HEUR_{670}$ aqueous solutions.

The DLS data for the HEURs with the smaller spacing, $EO_{195,}$ are illustrated in Figure 7. The trends noted with the larger EO spacings are observed (i.e., aggregate sizes increase with increasing concentrations); however, the median sizes are all smaller than their analogues with the larger EO spacing (Figures 5 and 6). With the smaller hydrophobe and smaller EO spacing, *b*-$C_{12}H_{26}$−$HEUR_{195,}$ there is no evidence of an association even up to 1.2 $\times$ 10^{-5} M (0.2 wt %) (Figure 7A), where fluorescence data (Figures 2 and 3) indicate there are associations. The smaller hydrophobe, (*b*-$C_{12}H_{24}$−$HEUR_{195}$, exhibits a bimodal distribution at 7.3 $\times$ 10^{-4} M (0.6 wt %, Figure 7C) and they grow marginally in size with concentration, up to 1.2 $\times$ 10^{-3} M (1.0 wt %, Figure 7E), well above the concentration where the pyrene emission ratio, I_1/I_3, levels off.

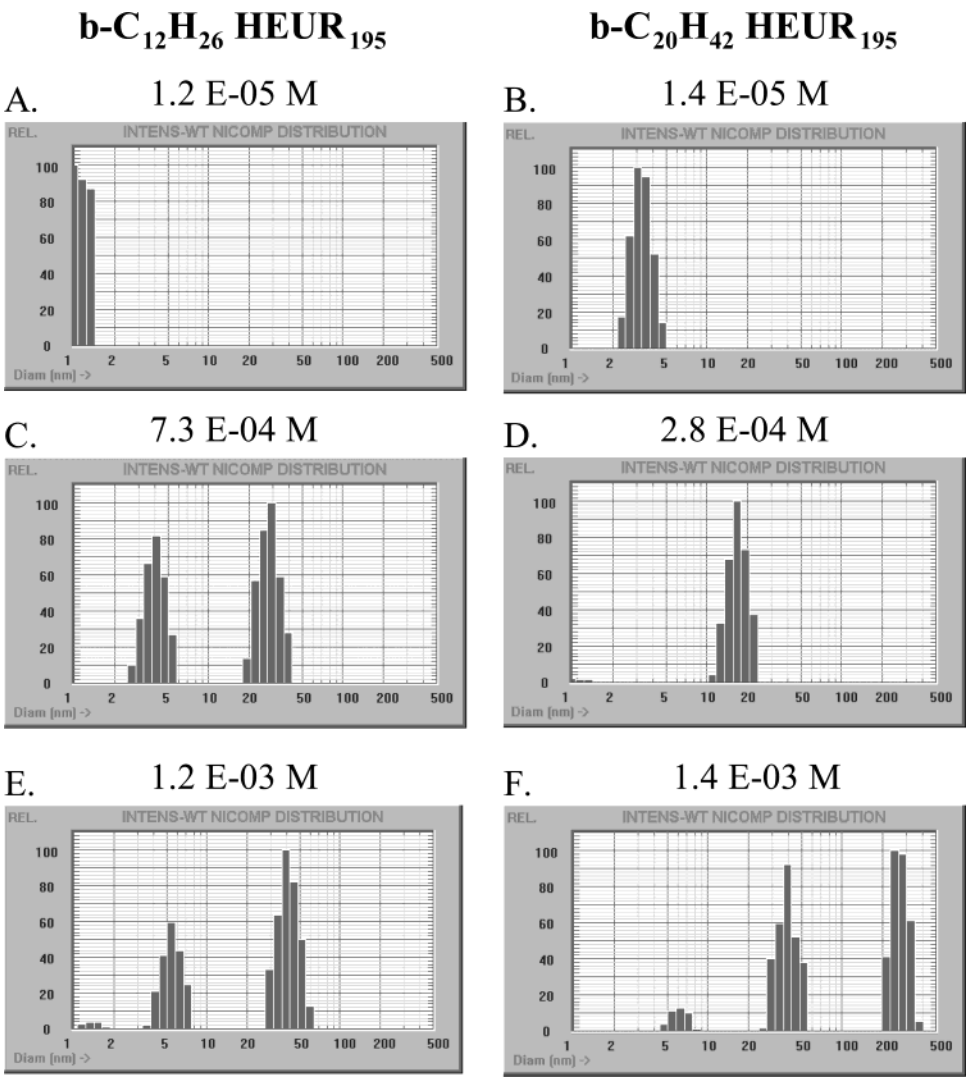

Figure 7. Median aggregate sizes for aqueous R−H_{12}MDI−$HEUR_{195}$ solutions at different concentrations.

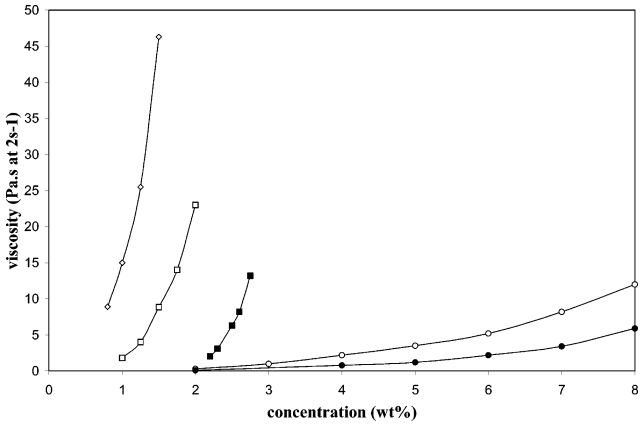

Figure 8. Low shear rate (2 s^{-1}) viscosity as a function of HEUR thickener concentration (wt %). (◇) (*l*-$C_{12}H_{25}$−H_{12}MDI)$_2$−POE_{670}; (□) (*b*-$C_{16}H_{34}$−H_{12}MDI)$_2$−POE_{670}; (■) (*b*-$C_{16}H_{34}$−H_{12}MDI)$_2$−$HEUR_{195}$; (○) (*b*-$C_{12}H_{25}$−H_{12}MDI)$_2$−POE_{670}; (●) (*b*-$C_{12}H_{25}$−H_{12}MDI)$_2$−POE_{195}.

The more hydrophobic analogue, *b*-$C_{20}H_{42}$−$HEUR_{195}$, does associate at a 1.4 × 10^{-5} M (0.01 wt %) concentration; a median aggregate size of 3 nm (Figure 7B) is observed. At this size the aggregate would be the intrahydrophobic association noted[38] in the pyrene labeled POE_{100} and POE_{200} studies. This median aggregate size is not observed in the larger EO spacing.

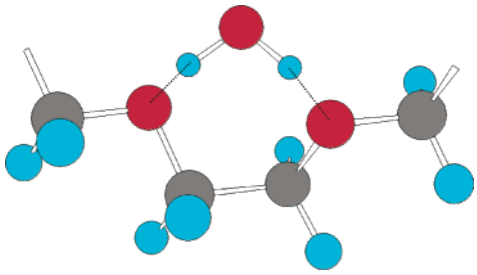

Figure 9. Trans−gauche−trans conformation of POE, with an associating H_2O molecule.

With increasing concentration, the aggregate size of *b*-$C_{20}H_{42}$−$HEUR_{195}$ increases to a median size just below 20 nm at 0.1 (0.2 wt %, Figure 7D). At the higher concentration, the largest median diameter aggregate with the larger hydrophobe, *b*-$C_{20}H_{42}$−$HEUR_{195}$, is just over 200 nm (Figure 7F). This is half the value of the larger aggregate with greater POE spacing (*b*-$C_{20}H_{42}$−$HEUR_{670}$) solutions at 0.4 wt % (Figure 6D), where significant viscosity increases are observed. Significant increases in viscosity in *b*-$C_{20}H_{42}$−$HEUR_{195}$ solutions are not observed until a concentration of 2.0 wt % is approached. At this concentration, 1.4 × 10^{-3} M, the largest median size approaches 500 nm, as observed in the larger EO spacing, when a significant viscosity increase is observed with increasing

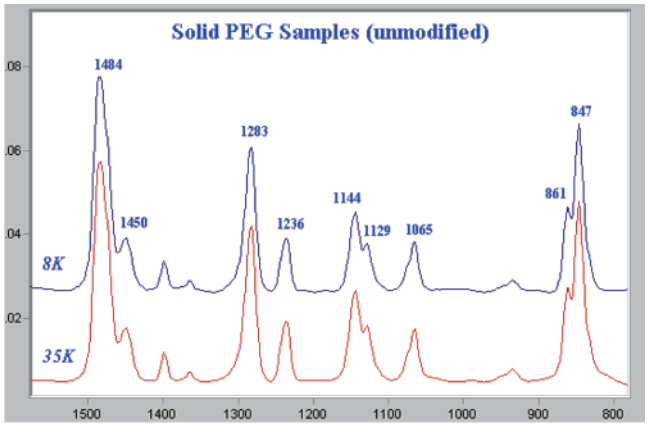

Figure 10. Raman spectra of POE_{670} (35K) and POE_{195} (8K) samples in the solid state.

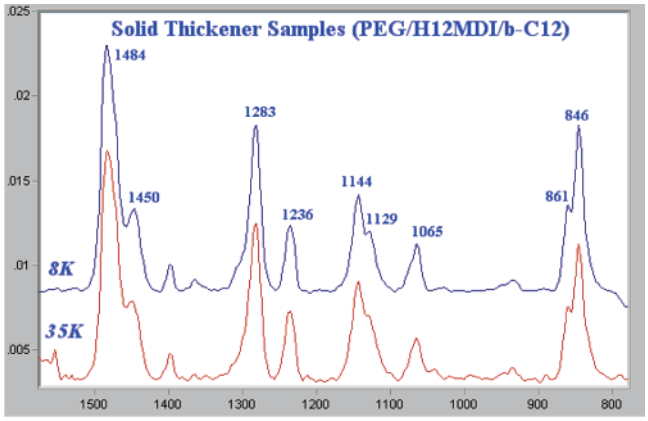

Figure 11. Raman spectra of hydrophobically modified POE samples, $(b\text{-}C_{12}H_{26}H_{12}MDI)_2-POE_{670}$ and $(b\text{-}C_{12}H_{26}H_{12}MDI)_2-POE_{195}$, in the solid state.

concentration. There are parallels in these data with the viscosity increases noted in the viscosity section.

D. Effect of Hydrophobe Structure on Solution Viscosity. Our prior synthesis[6] of uni-HEURs involved the direct addition of octadecyl monoisocyanate to poly(ethylene glycol)s (POE). This procedure does not allow for the synthesis of branched hydrophobes. In the synthesis of branched-terminal hydrophobes, the step-growth synthesis was avoided by adding a large excess of $H_{12}MDI$ (which contributes to the effective terminal hydrophobe size of the linear or branched hydrophobe) to POE and then adding the desired hydrophobe to the terminal isocyanate on the modified POE. This reaction (Scheme 1) provides a mixture of unreacted diisocyanates and POEs with terminal isocyanates. After addition of the amine or alcohol this mixture requires a more extensive rectification to remove the low molecular species than the direct addition of monoisocyanates to POE. The use of $H_{12}MDI$ adds to the difficulty in obtaining a clean HEUR, because it is a mixture of 3- and 4-isomeric positioned isocyanates and the alicyclic substituents are a mixture of equatorial−equatorial and equatorial−axial isomers. With all its deficiencies, the use of $H_{12}MDI$ as the diisocyanate produces large "effective" terminal hydrophobe HEURs, with intermediate hydrophobe sizes. In the synthesis of narrow molecular weight "uni"-HEURs in this study, an impurity (the direct addition of two alcohols to $H_{12}MDI$) is generated during the reaction of the hydrophobic alcohol with the isocyanate-terminated PEO. If this impurity is not removed, the linear $C_{12}H_{25}-H_{12}MDI-HEUR_{670}$ is less viscosifying than the branched. An extra extraction of the HEUR with methanol is required to remove this byproduct from the linear HEUR. When this is done and the largest aliphatic diisocyanate is used as the coupler, the solutions observed with the linear $(C_{12}H_{25}-H_{12}MDI)_2-POE_{670}$ are more viscous than those with the $(b\text{-}C_{16}H_{34}-H_{12}MDI)_2-POE_{670}$ HEUR thickener.

As the concentration is increased beyond that permissible in fluorescence and DLS, the differences in the viscosifying efficacy of linear vs branched hydrophobe equivalents is evident (Figure 8). The linear hydrophobe in the hydrophobic equivalent comparison $((l\text{-}C_{12}H_{25}-H_{12}MDI)_2-POE_{670}$ vs $(b\text{-}C_{16}H_{34}-H_{12}MDI)_2-POE_{670})$ is more viscosifying. The thixotropy and shear thinning noted in these HEURs became excessive with the larger hydrophobes, $l\text{-}C_{16}H_{33}-$ and $(b\text{-}C_{20}H_{42}-H_{12}MDI)_2-POE_{670}$ HEURs, and their tendency to gel at concentrations approaching the onset of viscosity increases made it difficult to assess the relative ability of these large linear vs branched terminal hydrophobes to build viscosity. We elected to revisit these large linear and branched hydrophobes in the multibranched terminal hydrophobe studies in the next article, where a less hydrophobic diisocyanate, hexamethylene diisocyanate, is used to couple the hydrophobes to POE_{670}. The smaller $(b\text{-}C_{12}H_{25}-H_{12}MDI)_2-$POEs studied in the Raman section to follow were Newtonian fluids.

Raman Spectroscopy of POE and HEUR Aqueous Solutions

Raman spectroscopy is an attractive technique because it is very sensitive to small changes in microstructure and it offers the ability to study polymer conformations in aqueous solution where the water spectrum is weak and does not obscure any of the conformation bands. The Raman spectrum of POE has been studied extensively, making it especially applicable to model HEUR aqueous solutions that are compositionally >95% POE. A variety of techniques including X-ray,[41] NMR,[42] and IR have concluded that the conformation of POE in the crystalline state is helical, containing seven chemical units and two fiber turns in a fiber identity period of 19.3 Å.[43,44] In the crystalline state, the preferred conformation of the POE repeat unit is trans−gauche−trans (TGT, Figure 9, without the H_2O molecule).

In the melt phase and in chloroform solutions, the conformation of POE (IR[45,46] and Raman[47−51]) loses its helical structure and is disordered in a number of new conformations (TGG, GGG, TTT, TTG, or GTG); however, in aqueous solutions spectral analysis reveals that POE, although more disordered than in the solid state, retains the TGT conformation to a large degree. The TGT state is the lowest energy conformation for water to bind to the oxygen ether linkages (Figure 9). In extremely dilute (<0.03 mole fraction) solutions, this trend reverses and a more disordered structure prevails.

These results led others to examine the conformation of the oxyethylene chain in aqueous surfactant solutions[52−55] since the micellization and solubilization of the surfactants are closely related to the conformational states of the hydrophobic and the hydrophilic oxyethylene moieties. The systematic study of Matsuura et al. concluded that the gauche conformation of the oxyethylene chain is more favored than the trans conformation with increasing water addition. It was again concluded

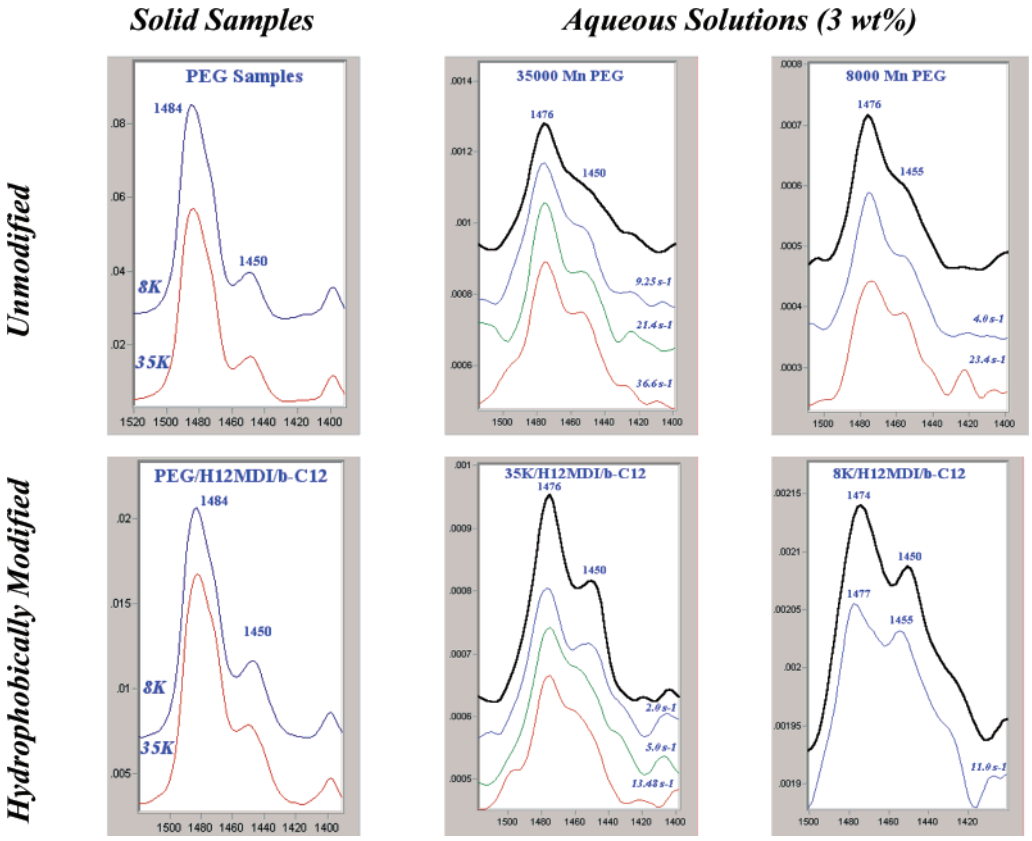

Figure 12. Raman spectra in the region 1500−1400 cm^{-1} in solid form (left graphs), in stagnate aqueous solutions [upper spectra (in center and right spectra)], and in solutions under shear deformation (shear rates are listed on lower right of spectra).

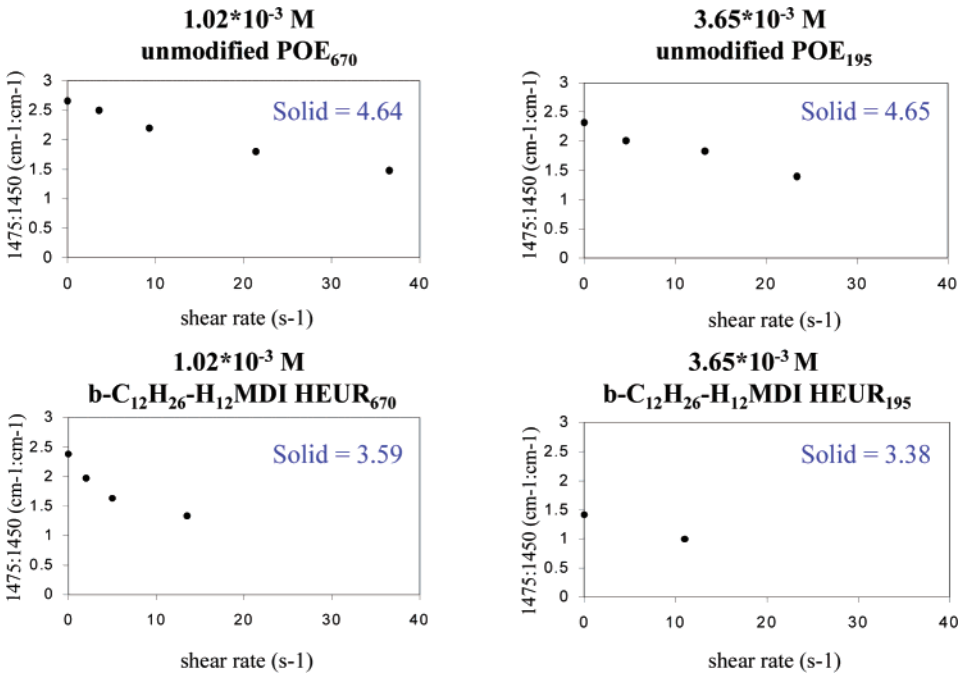

Figure 13. Degree of disorder (1475:1450 cm^{-1}) for POE and HEUR thickeners at different shear rates.

that the increased stabilization of the gauche conformation is most likely caused by hydrogen bonding between the ether oxygens in the oxyethylene chain and water molecules (Figure 9).

In this section we attempt to apply past Raman conformational analyses of POE, in aqueous solution, to uni-HEUR solutions, under both stagnant and low shear deformation conditions. The least hydrophobic (*b*-$C_{12}H_{26}$−H_{12}MDI)$_2$−POE) HEURs are examined to minimize viscosity effects (Figure 8). In carbon equivalencies the *b*-$C_{12}H_{26}$ group is equivalent to a linear C_9H_{19} hydrophobe. This is just above the minimum number of carbons, C_8H_{17}, necessary in a surfactant structure to form micellar aggregates. The association is assisted, in a structure containing so many oxyethylene units, by the terminal H_{12}MDI unit coupling the hydrophobe to POE. This specific hydrophobe was chosen as it permitted the use of higher concentrations (3 wt %) to

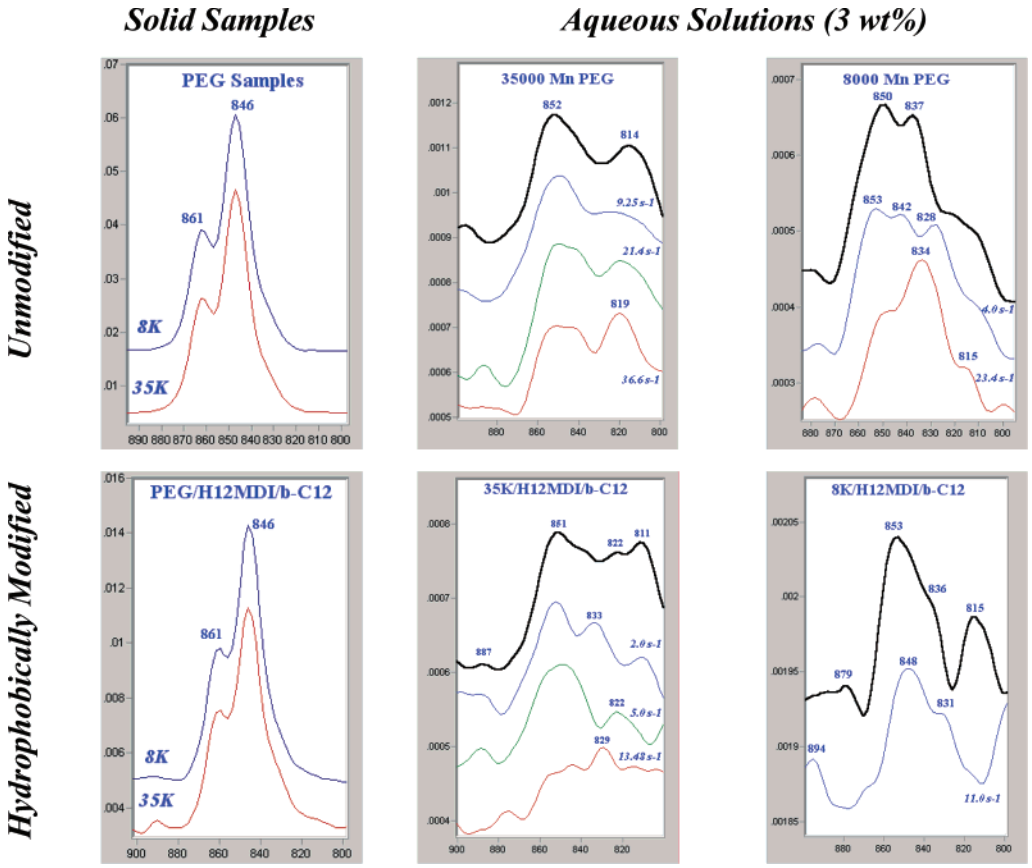

Figure 14. Raman spectra in the region 900−800 cm^{-1} in solid form (left graphs), in stagnate aqueous solutions [upper spectra (in center and right spectra)], and in solutions under shear deformation (shear rates are listed on lower right of spectra).

improve the Raman signal-to-noise ratio, while still maintaining an acceptable low viscosity level to minimize air entrapment with the pumping apparatus illustrated in Figure 1. Larger hydrophobe HEURs could not be run at 3 wt %, necessary to achieve a good signal-to-noise ratio, without high viscosities and air entrapment during the experimental study.

Raman spectra of solid unmodified POE_{670} and POE_{195} (commercial designations of 35K and 8K are used for identification in some of the Raman graphs, as is the symbol PEG) are illustrated in Figure 10. There is a small difference between the unmodified and the hydrophobically modified POEs (Figure 11), but all exhibit narrow and well-defined peaks typical of solid, crystalline samples. Sections of these spectra will be discussed in detail below.

Flow Experiments. The spectra of HEUR samples in aqueous solution (3 wt % with 2 mM SDS) are compared below with the solid sample spectra in three spectral regions, 1500−1400, 900−800, and 1320−1220 cm^{-1}, known to provide information on the conformation of the POE backbone.

A. 1500−1400 cm^{-1} (CH_2 Scissoring). Raman spectra in the 1500−1400 cm^{-1} region are illustrated in Figure 11. There are two narrow, well-defined peaks in the solid samples. The peak at 1484 cm^{-1} corresponds to the preferred TGT ordered structure for the $O-CH_2-CH_2-O$ bonds. The peak at 1450 cm^{-1} corresponds to a trans conformation of the CH_2-CH_2 bond, giving a TTT structure for the $O-CH_2-CH_2-O$ bonds (i.e., disordered or amorphous region). The ratio of these two Raman bands (Figure 12) is a measure of the amount of order/disorder in the system. The solid samples of unmodified POE_{195} (4.65) and POE_{670} (4.64) have a similar degree of ordering. The addition of hydrophobes increases the disorder in the solid system by disrupting the ability of the POE chains to pack as efficiently. The (b-$C_{12}H_{26}$-$H_{12}MDI)_2$-POE_{670} is less disordered than the (b-$C_{12}H_{26}$-$H_{12}MDI)_2$-POE_{195} (3.59 vs 3.38) in the solid samples. This would be expected due to the larger number of hydrophobes per weight for the smaller oxyethylene spacing (approximately 3.5 times on a molar basis).

Upon addition of these polymers to water, the crystal structure is disrupted (loss of helix) and the Raman bands are broadened, while other bands are split, and some new bands appear (Figure 12). This loss of order is reflected in the 1484 (which shifts to 1475) and 1450 cm^{-1} band ratios. For all four samples, unmodified and hydrophobically modified, there is significant disordering; however, throughout all of the transition, the dominance of the 1475 cm^{-1} peak remains, indicating the preference of the TGT conformation. This is expected since water will bind to the POE backbone in the lowest energy conformation. Hydrophobic modification of POE results in a greater degree of disorder in the POE backbone in aqueous solution than with unmodified POE.

With shear deformation of the fluids the preferred TGT conformation decreases, in all solutions. In the unmodified POE solutions a measure of disorder of 1.5 (the ratio of the peak heights of 1575 and 1450 cm^{-1} bands) is achieved above 30 s^{-1} (Figure 13). The (b-$C_{12}H_{26}$-$H_{12}MDI)_2$-POE_{670} solution exhibits a decrease in the 1475:1450 cm^{-1} ratio at lower shear rates and then plateaus at a ratio of 1.5 around 11 s^{-1}. With the small b-$C_{12}H_{26}$ hydrophobes, the samples display essentially Newtonian rheology over the shear rates examined (not shown), yet the application of shear

stress results in an increased amount of disordered conformations as reflected by a decrease in the 1475:1450 cm^{-1} ratios (Figure 13). The high degree of disorder in the low molecular weight unperturbed HEUR may reflect the intrahydrophobic bonding (i.e., the cherished flowered micelle conformation).

B. 900−800 cm^{-1} (C−O Stretch and CH_2 Rocking). In this spectral region, the solid samples of unmodified and hydrophobically modified POE display two sharp, well-defined bands at 861 and 846 cm^{-1} (Figure 14). Both have been equated with the TGT conformation of the $O-CH_2-CH_2-O$ bonds. It has been shown in previous work that upon dissolution of POE into water these two bands coalescence into a single, broad band near 850 cm^{-1}. Normal coordinate analysis of this region for aqueous solutions of POE suggests that a prominent band at 850−855 cm^{-1}, with a possible shoulder at 832−834 cm^{-1}, is associated with the gauche conformation of the OCH_2-CH_2O segment, while the band at 808−823 cm^{-1} is associated with the same segment in the trans conformation.

The most striking observation in the spectra is that the higher molecular weight samples exhibit more disorder in solutions at rest than observed with either low molecular weight. This is not indicated in the $-CH_2-$ scissoring spectra (1500−1400 cm^{-1}). The greater degree of disorder in the higher molecular weight is not unusual: a greater degree of order in lower molecular weight HEC and xanthan gum, than in these respective polymers of higher molecular weight, has been observed by light scattering and viscosity measurements.[56,57] The disorder increases significantly in POE_{670} with increasing shear rate so that the TGT conformer is not the preferred conformation. This extent of disorder is not reflected in the 1500−1400 cm^{-1} spectra with increasing shear rate. The $HEUR_{670}$ is highly disordered in stagnant solutions. The degree of disorder with increasing shear rate cannot be estimated with both $HEUR_{670}$ and $HEUR_{195}$ due to shifting of the 815 cm^{-1} band to lower frequencies than measured.

C. 1320−1220 cm^{-1} (CH_2 Twisting). There is a third region (at an intermediate frequency, 1320−1220 cm^{-1}) that has been reported to discriminate between POE segment conformations. The solid samples of unmodified and hydrophobically modified POE display two narrow, well-defined bands in the 1320−1220 cm^{-1} region at 1283 and 1236 cm^{-1}. The band at 1283 cm^{-1} is indicative of the TGT structure, while the band at 1236 cm^{-1} is a combination of structures (TGT, TTT, TTG). Upon dissolution of the POEs and HEURs into water at 3 wt %, the spectra become extremely complex. Quantitative comparisons to the solid samples cannot be made in this region since the bands used to observe the amount of order/disorder in the POE backbone are the result of very broad splitting or new band formation in water.

Conclusions

Observations among low molecular weight surfactants indicate that linear hydrophobes form micellar aggregates at lower concentrations than branched hydrophobes of "equivalent hydrophobicity (EH)". Hydrophobes attached to relatively large oxyethylene (EO) chains might not be expected to follow conventional surfactant behavior because of the steric restrictions of the POE spacers on their associations. Nevertheless, the placement of the different hydrophobes on POE terminal positions produces marked differences in the HEUR's ability to viscosify with increasing hydrocarbon size. In the comparison of EH hydrophobes of moderate size, the linear hydrophobe produces higher viscosities than dibranched hydrophobe HEURs.

The I_1/I_3 ratio at higher HEUR concentrations reflects a difference in hydrophobicity between the linear and branched hydrophobes, consistent with the relative hydrophilicity of branched hydrophobes noted in the review of conventional surfactant in the Introduction. The I_1/I_3 ratio at high concentrations is related to the relative viscosity build within the linear or branched hydrophobe HEURs, but the influence of the hydrophilicity of the branched hydrophobes negates a relationship with viscosity build across both HEUR families.

Dynamic light scattering studies indicate that the onset of viscosity build begins as the aggregate size approaches 500 nm. This is influenced by the spacer length and hydrophobe size. For example, the smaller hydrophobe (b-$C_{12}H_{24}-H_{12}$MDI−POE_{195}) HEUR exhibits marginal growth size with concentration up to 1.2 $\times$ 10^{-3} M, well beyond the concentration where the pyrene emission ratio exhibits its upper level plateau. The results are reflective of intrahydrophobic bonding (supported by the Raman spectra in the CH_2 scissoring region (1500−1400 cm^{-1})). A larger hydrophobe (e.g., b-$C_{20}H_{42}-H_{12}$MDI−POE) HEUR, with an increased residence time in micellar aggregates, is more effective in building networks, particularly with larger POE spacer units, and the aggregate size approaches that needed for viscosity build at lower HEUR concentrations.

In the Raman spectra the loss of the preferred trans−gauche−trans conformer for hydration decreases with increasing shear rate up to 30 s^{-1} for Newtonian fluids. This would contribute to the shear-induced phase separation observed by several investigators. Rheooptical studies[58] of the larger hydrophobe (b-$C_{20}H_{42}-H_{12}$MDI)$_2$−POE_{xxx} HEURs to obtain shear-thinning solutions could not be studied meaningfully without the presence of surfactant due to gel formation. The (b-$C_{20}H_{42}-H_{12}$MDI)$_2POE_{670}$ at 0.7 wt % was studied in 6.15 mM SDS solutions; (b-$C_{20}H_{42}-H_{12}$MDI)$_2POE_{195}$ at 1.7 wt % was studied in 12.3 mM SDS solutions. Orientation of the polymers (>70%) is achieved by 20 s^{-1}, and the birefringence, a measure of segmental orientation, increases up to this shear rate. Both observations complement the shear rate limit noted in the Raman study. Much could be learned from a continued tandem use of these two techniques, particularly under Coulette flow, where air entrapment could be minimized.

References and Notes

(1) May, R.; Kaczmarski, J. P.; Glass, J. E. *Macromolecules* **1996**, *29* (13), 4745.
(2) Glass, J. E. *Hydrophilic Polymers, Performance with Environmental Acceptability*; Advances in Chemistry Series 248; American Chemical Society: Washington, DC, 1996.
(3) Glass, J. E. *J. Coatings Technol.* **2001**, *73* (913), 1−24.
(4) Lundberg, D. J.; Glass, J. E.; Eley, R. R. *Proc. ACS Div. Polym. Mater.: Sci., Eng.* **1989**, *61*, 533.
(5) Lundberg, D. J.; Brown, R. G.; Glass, J. E.; Eley, R. R. *Langmuir* **1994**, *10* (9), 3027.
(6) Kaczmarski, J. P.; Glass, J. E. *Macromolecules* **1993**, *26*, 5149.
(7) Kaczmarski, J. P.; Glass, J. E. *Langmuir* **1994**, *10* (9), 3035.
(8) Kaczmarski, J. P.; Tarng, M.-R.; Ma, Z.; Glass, J. E. *Colloids Surf., A* **1999**, *147*, 39.
(9) Graciaa, A.; Fortney, L. N.; Schechter, R. S.; Wade, W. H.; Yiv, S. *Soc. Pet. Eng. SPE* **1980**, 5815.

(10) Abe, M.; Schechter, D.; Schechter, R. S.; Wade, W. H.; Weerasooriya, U.; Yiv, S. *J. Colloid Interface Sci.* **1986**, *114* (2), 342.
(11) Bracket, Y.; Fortney, L. N.; Schechter, R. S.; Wade, W. H.; Yiv, S. H. *J. Colloid Interface Sci.* **1983**, *92* (2), 561.
(12) Varadaraj, R.; Bock, J.; Zushma, S.; Brons, N. *Langmuir* **1992**, *8*, 14.
(13) Varadaraj, R.; Bock, J.; Valint, P.; Zushma, S.; Brons, N. *J. Phys Chem.* **1991**, *95*, 1677.
(14) Varadaraj, R.; Schaffer, H.; Bock, J.; Valint, P., Jr. *Langmuir* **1990**, *6*, 1372.
(15) Varadaraj, R.; Bock, J.; Valint, P., Jr.; Brons, N. *Langmuir* **1990**, *6*, 1376.
(16) Rosen, M. J. *Surfactants and Interfacial Phenomena*, 2nd ed.; John Wiliey & Sons: New York, NY, 1989.
(17) Kingston, B. H.; Gary, J. J.; Hellwig, W. B. *Anal. Chem.* **1969**, *41* (1), 86.
(18) Vorobyova, O.; Winnik, M. A. Associative Polymers in Aqueous Media; Glass, J. E., Ed.; ACS Symposium Series 765; American Chemical Society: Washington, DC, 2000; Chapter 9.
(19) Zana, R. In *Surfactant Solutions*; Zana, R., Ed.; Marcel Dekker: New York, 1987; Vol. 22, p 241.
(20) Grieser, F.; Drummond, C. J. *J. Phys. Chem.* **1988**, *92*, 5508.
(21) Turro, N. J.; Yekta, A. *J. Am. Chem. Soc.* **1978**, *100*, 5951.
(22) Warr, G. G.; Grieser, F. *J. Chem. Soc., Faraday Trans.* **1986**, *1*, 1813.
(23) Lissi, E. A.; Abuin, E. *J. Colloid Interface Sci.* **1985**, *105*, 1.
(24) Witte, F. M.; Engberts, J. B. F. N. *Colloids Surf.* **1989**, *36*, 417.
(25) Winnik, F. M.; Winnik, M. A. *Polym. J.* **1990**, *22* (6), 482.
(26) Nilsson, S. *Macromolecules* **1995**, *28*, 7837.
(27) Evertsson, H.; Nilsson, S.; Holmberg, C.; Sundelof, L. O. *Langmuir* **1996**, *12*, 5781.
(28) Zana, R.; Binana-Limbele, W.; Kamenka, N.; Lindman, B. *J. Phys. Chem.* **1992**, *96*, 5461.
(29) Lianos, P.; Zana, R. *J. Phys. Chem.* **1980**, *84*, 3339.
(30) Almgren, M.; Lofroth, J. E. *J. Colloid Interface Sci.* **1981**, *81*, 486.
(31) Malliaris, A. *Prog. Colloid Polym. Sci.* **1987**, *73*, 161.
(32) Nilsson, S.; Holmberg, C.; Sundelof, O. *Colloid Polym. Sci.* **1995**, *273*, 83.
(33) Wikander, G.; Johansson, L. B. A. *Langmuir* **1988**, *5*, 728.
(34) Magny, B.; Iliopoulos, I.; Zana, R.; Audebert, R. *Langmuir* **1994**, *10*, 3180.
(35) Alami, E.; Almgren, M.; Brown, W.; Francois, J. *Macromolecules* **1996**, *29*, 2229.
(36) Alami, E.; Abrahmsen-Alami, S.; Vasilescu, M.; Almgren, M. *J. Colloid Interface Sci.* **1997**, *193*, 152.
(37) Alami, E.; Rawiso, M.; Isel, F.; Bienert, G.; Binana-Limbele, W.; Francois, J. *Hydrophilic Polymers: Performance with Environmental Acceptance*; Glass, J. E., Ed.; Advances in Chemistry Series 248: American Chemical Society, Washington, DC, 1995; Chapter 18.
(38) Char, K.; Frank, C. W.; Gast, A. P.; Tang, W. T. *Macromolecules* **1987**, *20*, 1833.
(39) Pham, Q. T.; Russel, W. B.; Thibeault, J. C.; Lau, W. *Macromolecules* **1999**, *32*, 2996.
(40) Devanand, K.; Sesler, J. C. *Macromolecules* **1991**, *24*, 5944.
(41) Tadokoro, H.; Chatani, Y.; Yoshihara, T.; Tahara, S.; Murahashi, S. *Makromol. Chem.* **1964**, *73*, 109.
(42) Liu, K.; Parsons, J. *Macromolecules* **1969**, *2*, 529.
(43) Yoshihara, T.; et al. *J. Chem. Phys.* **1964**, *41*, 2902.
(44) Miyazawa T.; et al. *J. Chem. Phys.* **1963**, *37*, 2764.
(45) Matsuurw, H.; Sagawa, T. *J. Mol. Liq.* **1995**, *65/66*, 313.
(46) Begum, R.; Matsuura, H. *J. Chem. Soc.* **1997**, *93* (21), 3839.
(47) Koenig, J.; Anwood, A. C. *J. Polym. Sci.* **1970**, *8*, 1787.
(48) Maxfield, J.; Shepherd, I. W. *Polymer* **1975**, *16*, 505.
(49) Matsuura, H.; Fukuhara, K. *J. Polym. Sci.: Part B* **1986**, *24*, 1383.
(50) Yoshida, H.; et al. *J. Mol. Struct.* **1994**, *311*, 205.
(51) Masatoki, S.; et al. *Chem. Lett.* **1995**, 991.
(52) Kalyanasundaram, K.; Thomas, J. K. *J. Phys. Chem.* **1976**, *80* (13), 1462.
(53) Matsuura, H.; Fukuhara, K. *J. Mol. Struct.* **1985**, *126*, 251.
(54) Matsuura, H. *Trends Phys. Chem.* **1990**, 89.
(55) Matsuura, H.; et al. *J. Phys. Chem.* **1991**, *95*, 10800.
(56) Foweraker, A. R.; Jennings, B. R. *Makromol. Chem.* **1977**, *178*, 506.
(57) Holzwarth, G. *Carbohydr. Res.* **1978**, *66*, 173.
(58) Elliott, P. T.; Matthies, M. O.; Wetzel, W. H.; Kulicke, W. M.; Glass, J. E. *Proc. ACS Div. Polym. Mater.: Sci., Eng.* **2001**, *85*, 211.

MA020166F